[Discrete and continuous models for static and modal analysis of out of plane loaded masonry - ScienceDirect](https://www.sciencedirect.com/science/article/abs/pii/S0045794917301669?via%3Dihub)

Link to publisher version:

https://www.sciencedirect.com/science/article/abs/pii/S0045794917301669?via%3Dihub

DOI:

https://doi.org/10.1016/j.compstruc.2017.03.015

Discrete and Continuous Models for Static and Modal Analysis of Out of Plane Loaded Masonry

D. Baraldi[1], A. Cecchi[2]

Department of Architecture Construction Conservation DACC, Università IUAV di Venezia, Italy

[1] **danielebaraldi@iuav.it**
[2] **cecchi@iuav.it**

Abstract

A critical review of analytical and numerical models for studying masonry out of plane behaviour is presented. One leaf historical masonry, composed by rigid blocks arranged regularly with dry or mortar joints, is considered. Discrete model with rigid blocks, Love-Kirchhoff and Reissner-Mindlin plate models and 3D heterogeneous FEM are adopted. An existing simple and effective discrete model is adopted and improved by applying matrix structural analysis techniques for static and modal analysis of masonry walls in the elastic field, but the formulation allows to account for material nonlinearity. Elastic parameters of both plate models are based on an existing compatible identification between 3D discrete model and 2D plate models. Static and modal analysis of masonry walls with several boundary conditions are carried on, numerical tests account for in plane size of heterogeneity and structure thickness by means of in and out of plane scale factors. Results show that discrete model is simple and effective for representing masonry behaviour, especially when size of heterogeneity is smaller than overall panel size. Decreasing in plane scale factor, plate models converge to the discrete one, but the Reissner-Mindlin one shows a better convergence and also allows adopting a simple FE for performing numerical analysis.

Keywords: masonry, out of plane analysis, modal analysis, discrete model, Kirchhoff plate, Mindlin plate~~, heterogeneous material, homogenisation, elasticity~~.

1 Introduction

Masonry is a structural material obtained by composition of natural or artificial blocks connected by dry or mortar joints. For this type of material, size of heterogeneity (or size of block) is often not negligible with respect to the global size of a structural element; then, several ad-hoc models have been developed in the last decades adopting different approaches.
The model that may appear as the more simple one among others for representing masonry behaviour is a heterogeneous Finite Element (FE) model. The first example of such a model type was limited to the in plane case, characterised by blocks modelled with FE quadrilateral elements and joints modelled with one-dimensional elements [1,2]. Small improvements of these initial works were performed by Tzamtzis & co-workers by defining three-dimensional elements and joints, but limiting the field of analysis to the in plane case [3,4]. However, the limits of this approach are represented by the large number of degrees of freedom involved and the consequent computational effort for the analysis of macro-scale problems.
Another class of numerical models frequently adopted for representing masonry behaviour is discrete modelling, that is characterised by rigid or deformable elements in contact, in order to represent natural or artificial blocks in contact by means of dry or mortar joints. Into this class of models, the discrete element method (DEM) is one of the most representative approaches. Such a method is characterised by distinct elements, with finite size and independent degrees of freedom, that can be subject to finite displacements and rotations; moreover, contacts between elements can vary during analysis and are automatically recognized by the model. DEM had been introduced by the pioneering works of Cundall in the field of rock mechanics [5,6], that started considering the plane case and created the well-known program UDEC [7], and continued modelling three-dimensional problems [8,9], creating the program 3DEC [10]. Several developments in the DEM field are represented by the combination of discrete and finite elements [11,12] accounting for block deformability; however these models are still limited to in plane analysis. Another type of discrete models is represented by those adopted in Discrete Deformation Analysis (DDA, [13]) that are characterised by deformable blocks by means of uniform strain and stresses in plane state. This model was extended to the 3D case even if at preliminary stage [14,15].
The discrete models cited above were created for modelling granular materials and for studying rock mechanics, in several cases such models were extended to the field of masonry structures with results comparable with those obtainable with other classes of models; the work of Lemos [16] presents a deep review of DEM applied to masonry structures, furthermore the recent book edited by Bagi, Sarhosis and Milani [17] collects an up-to-date review of DEM for masonry and other discrete approaches.
However, historical masonry is frequently made of strong and rigid natural or artificial blocks and weak, thin and deformable mortar joints. For this reason, numerical models, characterised by rigid blocks, with deformability concentrated at mortar joints or dry contacts, subject to small displacements that do not vary contact topology, should be sufficiently accurate and effective. Effectiveness is given by the

small number of degrees of freedom involved in the analysis that allows to model structures starting from small masonry panels to building facades and bridges. It is worth noting that these models cannot be defined DEMs but still remain discrete models. Considering the in plane case, this type of model was adopted by many authors in linear and non-linear fields [18-22]. In particular, the discrete and heterogeneous models introduced by Cecchi and Sab [20] were extended to the out of plane case by also performing homogenisation procedures [23-25]. Similarly, the 'rigid-body-spring-model' introduced by Casolo was effectively extended to the out of plane case, in linear and nonlinear fields [26,27] and it was also compared with a homogenised model [28].

Heterogeneous and discrete models are often linked with continuous materials equivalent to masonry, obtained by means of identification or homogenisation procedures. Continuous models are another class of models that are generally adopted for studying masonry behaviour at macroscale level, when both heterogeneous and discrete models start to be inapplicable due to the huge number of degrees of freedom involved in the analysis of masonry buildings. Considering the in plane case, standard Cauchy models were obtained applying periodic homogenisation techniques and considering the elastic behaviour of both brick and mortar [20,24,29]; moreover, micropolar or higher order continua were taken in consideration [30-35]. Considering the out of plane case, Stefanou et al. [36] performed a 3D Cosserat homogenisation of regular masonry composed by rigid elements in the linear elastic field and then proposed a FE formulation for Cosserat elastic plates [37]. However more generally, research in the 3D or out of plane field has been generally focused on nonlinear masonry behaviour for performing nonlinear, limit and stability analysis of walls, facades and buildings [27,38-46]. Recently, Ferreira et al. [47] presented an accurate literature review related to the analysis of unreinforced masonry out of plane loaded.

Considering the field of analysis based on homogenisation or identification procedures, plate models are often adopted for modelling out of plane masonry behaviour. In particular, the already cited works of Cecchi and Sab [23,24] show an identification procedure that is based on the balance of internal work in the discrete model and in the continuous one for a class of regular motions. In this field, an important problem is represented by how kinematic, dynamic and constitutive prescriptions of a discrete system are transferred to the continuous one. Hence, constitutive functions of the plate model may be different. For example, a Love-Kirchhoff plate model was proposed by Cecchi and Sab [20] for the case of both rigid and deformable blocks by means of homogenisation procedures, whereas Cecchi and Sab [24] studied both Love-Kirchhoff and Reissner-Mindlin plate models for rigid blocks connected by elastic interfaces by means of a 3D discrete model and homogenisation procedures.

Recently, Baraldi et al. [48] have presented a review of several numerical models, heterogeneous, discrete and continuous, that may be adopted for modelling the mechanical behaviour of masonry, with particular attention to out of plane loaded panels having a specific regular texture. The present work aims to extend the initial review by adding further information about out of plane displacement and rotation fields obtained with linear static analysis. Moreover, this work aims to extend the

campaign of numerical tests to the field of modal analysis, by means of a simple and effective approach for studying the discrete system, based on the determination of the stiffness matrix of the masonry assemblage. In addition, analytic solutions relative to natural frequencies of homogenised plates simply supported along edges are presented.
Hence in this work, numerical evaluation of the differences between a discrete model with rigid blocks, heterogeneous FEM and homogenised plate models is carried on for several case studies, performing static and modal analysis and considering several boundary conditions. The effect of varying in plane heterogeneity size (block width respect to panel width) is considered, as it has been done for the in plane case by several authors [32,35,49]; moreover, the effect of block aspect ratio (block width with respect to block height) and out of plane scale factor (block thickness with respect to panel width) are taken into account.
In order to represent the behaviour of historical masonry, characterised by block stiffness larger than mortar stiffness and joint thickness smaller with respect to block size, the discrete model adopted in this work and the corresponding homogenised plate models are based on the following hypotheses: i) masonry structure composed by infinitely rigid blocks subject to small displacements and with fixed contact topology, ii) mortar joints modelled as elastic interfaces. It is worth noting that the elastic behaviour considered may not be correct for studying masonry structures, given that such structures present a strong nonlinear behaviour even at low stress levels; however, the proposed review represents an initial step for performing numerical tests of out of plane loaded panels, that can be extended to the nonlinear field in further developments of this work, adopting, for example, a Mohr-Coulomb yield criterion for interface actions, following the numerical tests recently dealt with by authors both for the in and out of plane cases [50,51]. Moreover, the proposed campaign of modal analyses will allow to perform structural identification of masonry specimens by comparing numerical results with laboratory or in situ tests.

2 Discrete model

This work considers a regular and periodic masonry assemblage, characterised by equal rigid blocks arranged regularly with aligned horizontal joints and vertical joints staggered by block half width. This model is defined as Discrete Rigid Block Model (DRBM). A representative elementary volume (REV) is considered (Figure 1), characterised by a generic block $B_{i,j}$ surrounded by six blocks by means of six interfaces or joints S_{k_1,k_2}, with k_1, $k_2 = \pm 1$ for horizontal interfaces and $k_1 = \pm 2$, $k_2 = 0$, for vertical interfaces (Figure 1). Block dimensions are: a (height), b (width) and s (thickness). It is worth noting that this contact topology is assumed to be fixed during the analysis. Considering rigid block and small displacements hypothesis, the displacement of a generic block is represented by a rigid body motion referred to the motion of its centre and the rotation with respect to its centre:

$$\mathbf{u}^{i,j}(\mathbf{y}) = \mathbf{u}^{i,j} + \mathbf{\Omega}^{i,j}(\mathbf{y} - \mathbf{y}^{i,j}) \tag{1}$$

where $\mathbf{y}^{i,j}$ is the position of block centre in the Euclidean space and considering the out of plane case, $\mathbf{u}^{i,j} = u_3^{i,j}$ is the out of plane translation of block centre and $\mathbf{\Omega}^{i,j}$ is the rotation skew tensor collecting block rotations with respect to y_1 and y_2 axes:

$$\mathbf{\Omega}^{i,j} = \begin{bmatrix} 0 & 0 & \omega_2^{i,j} \\ 0 & 0 & -\omega_1^{i,j} \\ -\omega_2^{i,j} & \omega_1^{i,j} & 0 \end{bmatrix} \tag{2}$$

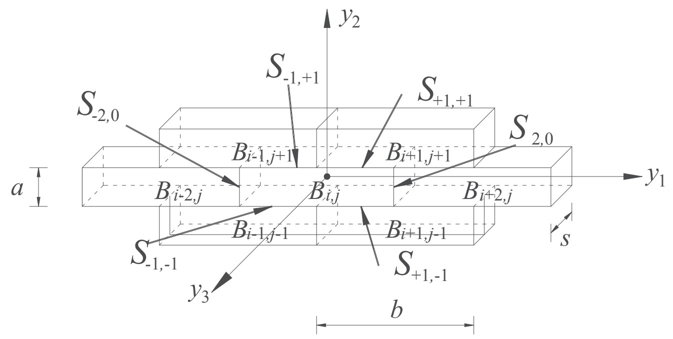

Figure 1. Discrete rigid block model (DRBM), running bond Representative Elementary Volume (REV)

Out of plane translation and rotations may be collected in $\mathbf{q}^{i,j} = \{u_3^{i,j}\ \omega_1^{i,j}\ \omega_2^{i,j}\}^T$. Following the procedure described by Cecchi and Sab [24] for the out of plane case, the interactions between two adjacent blocks $B_{i,j}$ and $B_{i+k_1,j+k_2}$ through a generic interface S_{k_1,k_2} are represented by unknown distribution of stresses, normal and tangential, $\sigma^{k_1,k_2} = \{\sigma_n^{k_1,k_2}\ \sigma_t^{k_1,k_2}\}^T$, with normal stress assumed positive in case of tension and negative in case of compression. Integrating stresses over the interface area, interface force $f_3^{k_1,k_2}$ and couples $c_1^{k_1,k_2}, c_2^{k_1,k_2}$ are obtained and collected in $\mathbf{f}^{k_1,k_2} = \{f_3^{k_1,k_2}\ c_1^{k_1,k_2}\ c_2^{k_1,k_2}\}^T$. Such stresses and interactions are related to the relative displacement and rotations between adjacent blocks, that are defined by:

$$\begin{aligned} d_3^{k_1,k_2} &= u_3^{i+k_1,j+k_2} - u_3^{i,j} + k_1 \frac{b}{2}\frac{(\omega_2^{i+k_1,j+k_2} + \omega_2^{i,j})}{2} - k_2 a \frac{(\omega_1^{i+k_1,j+k_2} + \omega_1^{i,j})}{2}, \\ \delta_1^{k_1,k_2} &= \omega_1^{i+k_1,j+k_2} - \omega_1^{i,j}, \\ \delta_2^{k_1,k_2} &= \omega_2^{i+k_1,j+k_2} - \omega_2^{i,j}, \end{aligned} \tag{3a-c}$$

and that may be collected in $\mathbf{d}^{k_1,k_2} = \{d_3^{k_1,k_2}\ \delta_2^{k_1,k_2}\ \delta_1^{k_1,k_2}\}^T$. Assuming the hypothesis of elastic interfaces, the constitutive relation that defines interaction between block $B_{i,j}$ and $B_{i+k_1,j+k_2}$ is $\sigma^{k_1,k_2}\mathbf{n}^{k_1,k_2} = \mathbf{K}^{k_1,k_2}\,\mathbf{d}^{k_1,k_2}$, where $\mathbf{n}^{k_1,k_2}$ is the vector normal to interface

S_{k_1,k_2}, and $\mathbf{K}^{k_1,k_2} = \mathrm{diag}\{K_t\ K_{c2}\ K_{c1}\}$ is the interface stiffness matrix, that collects tangential (K_t) and rotational (K_{c1}, K_{c2}) stiffness of the interface, that may be detailed for horizontal and vertical cases. Assuming mortar joints made of an isotropic and elastic material, interface stiffness values are function of mortar elastic modulus E^m and Poisson ratio ν^m. For instance:

$$K_t^h = K_{c2}^h = \frac{1}{e_v} \cdot \frac{E^m}{2(1+\nu^m)} = \frac{G}{e_v}, \quad K_{c1}^h = \frac{1}{e_v} \cdot \frac{E^m}{1-(\nu^m)^2} = \frac{K}{e_v}, \tag{4a,b}$$

$$K_t^v = K_{c1}^v = \frac{1}{e_v} \cdot \frac{E^m}{2(1+\nu^m)} = \frac{G}{e_v}, \quad K_{c2}^v = \frac{1}{e_v} \cdot \frac{E^m}{1-(\nu^m)^2} = \frac{K}{e_v}, \tag{5a,b}$$

where e_h, e_v represent horizontal and vertical joint thickness, respectively.

2.1 Elastic energy

The elastic energy over a generic interface is determined by defining the product of interface forces-couples and interface relative displacements-rotations:

$$\Pi_{k_1,k_2} = \frac{1}{2} \int_{S_{k_1,k_2}} (\sigma \mathbf{n})^T \mathbf{d}\, dS = \frac{1}{2} \int_{S_{k_1,k_2}} \mathbf{d}^T \mathbf{K}\, \mathbf{d}\, dS = \frac{1}{2} \mathbf{d}^T (\mathbf{KA})\, \mathbf{d} = \frac{1}{2} \mathbf{d}^T \overline{\mathbf{K}}\, \mathbf{d}, \tag{6}$$

where apex k_1,k_2 for vectors and matrices is omitted for simplicity, $\mathbf{A}$ is the generic diagonal matrix of area and inertias of the interface, that may be detailed for the horizontal case and for the vertical case: $\mathbf{A}_h = \mathrm{diag}\{S_h\ I_{h1}\ (I_{h1} + I_{h3})\}$, $\mathbf{A}_v = \mathrm{diag}\{S_v\ (I_{v2} + I_{v3})\ I_{v3}\}$, with:

$$\begin{aligned} &S_h = b\,s/2, \quad I_{h1} = b\,s^3/24, \quad I_{h3} = b^3 s/96, \\ &S_v = a\,s, \quad I_{v2} = a\,s^3/12, \quad I_{v3} = a^3 s/12. \end{aligned} \tag{7a-f}$$

Interface forces and couples may be obtained by differentiating the expression of interface elastic energy in Equation (6) with respect to each block displacement component. Then, extending such equation to the entire masonry assemblage (i.e. masonry panel), the total elastic energy Π is obtained and the subsequent equilibrium equation for the assemblage subject to out of plane actions $\mathbf{F}^{ext}$ is:

$$\mathbf{F}^{ext} = \partial \Pi_{panel} / \partial \mathbf{q} = \mathbf{K}^{panel} \mathbf{q}, \tag{8}$$

where $\mathbf{q}$ collects block degrees of freedom of the entire panel. Equation (8) may be solved by adopting a molecular dynamics algorithm or directly by explicitly defining the stiffness matrix of the entire assemblage $\mathbf{K}^{panel}$, extending to the out of plane case the procedure adopted by Baraldi and Cecchi [52] for the in plane case in the field of modal analysis of masonry panels. Details of the determination of $\mathbf{K}^{panel}$ may be found in appendix A.

2.2 Kinetic energy

The kinetic energy of a masonry assemblage may be defined at block level and it involves directly the global displacements of a generic block $\mathbf{q}^{i,j} = \{u_3^{i,j}\ \omega_2^{i,j}\ \omega_1^{i,j}\}^T$:

$$\Pi_{i,j}^{kin} = \frac{1}{2}[m(\dot{u}_3^{i,j})^2 + J_2(\dot{\omega}_2^{i,j})^2 + J_1(\dot{\omega}_1^{i,j})^2], \tag{9}$$

where $m = \gamma(a \cdot b \cdot s)$ is the mass of a block having density γ and $J_1 = m(a^2 + s^2)/12 = \gamma I_1$, $J_2 = m(b^2 + s^2)/12 = \gamma I_2$ are block polar or rotatory inertias with respect to y_1 and y_2 axes [24,36]. Mass and polar inertias of each block may be corrected by taking into account mortar joint thickness, especially if it is not standard (i.e. e_v or e_h > 10 mm), then m may be substituted by $m^* = \gamma[(a+e_v)\cdot(b+e_h)\cdot s]$, J_1 with $J_1{}^* = m^*[(a+e_h)^2 + s^2]/12$ and J_2 with $J_2{}^* = m^*[(b+e_v)^2 + s^2]/12$. Writing Equation (9) in matrix form, the (local) mass-polar inertia matrix $\mathbf{M}^{i,j}$ of the generic block may be highlighted:

$$\Pi_{i,j}^{kin} = \frac{1}{2}\{\dot{u}_3^{i,j} \quad \dot{\omega}_2^{i,j} \quad \dot{\omega}_1^{i,j}\}\begin{bmatrix} m & 0 & 0 \\ 0 & J_2 & 0 \\ 0 & 0 & J_1 \end{bmatrix}\begin{Bmatrix} \dot{u}_3^{i,j} \\ \dot{\omega}_2^{i,j} \\ \dot{\omega}_1^{i,j} \end{Bmatrix} = \frac{1}{2}(\dot{\mathbf{q}}^{i,j})^T \mathbf{M}^{i,j}\, \dot{\mathbf{q}}^{i,j}, \tag{10}$$

where $<\cdot> = d/dt$. The mass matrix of the entire panel $\mathbf{M}^{panel}$ is obtained by assembling the local mass matrix $\mathbf{M}^{i,j}$ over the panel, obtaining a diagonal mass matrix at panel level.

2.3 Modal analysis

The dynamic equilibrium of a masonry assemblage represented by a discrete model can be formulated by expressing the equilibrium of the effective forces associated with each of its degrees of freedom. Then, a multi degrees of freedom (MDOF) equilibrium equation is obtained [53]:

$$\mathbf{M}^{panel}\,\ddot{\mathbf{q}} + \mathbf{C}^{panel}\dot{\mathbf{q}} + \mathbf{K}^{panel}\,\mathbf{q} = \mathbf{F}^{ext}, \tag{11}$$

where $<\cdot\cdot> = d^2/dt^2$, $\mathbf{M}^{panel}$ and $\mathbf{K}^{panel}$ are, respectively, mass and stiffness matrices of the entire panel and $\mathbf{C}^{panel}$ is its damping matrix (a diagonal matrix collecting damping coefficients related to block DOFs). The equation above is coincident to the one adopted by the authors for solving static problems by means of a molecular dynamics algorithm [24,54] and that is usually adopted in more general

discrete element modelling numerical procedures. Such equation, in general, is solved by considering each DOF separately from other DOFs, hence it does not request the actual determination of panel matrices. On the other hand in this work, matrices definition is fundamental for performing static and modal analyses.
For simplicity, the equations of motion of a freely vibrating undamped system can be obtained by omitting the damping matrix and the applied load vector: $\mathbf{M}^{panel}\ddot{\mathbf{q}}+\mathbf{K}^{panel}\mathbf{q}=\mathbf{0}$. Then, assuming that the free vibration motion of the panel is simple harmonic, which may be expressed for a MDOF system as $q_i(t)=q_i\sin(\eta t+\theta)$, the equation of motion is modified as - $-\eta^2\mathbf{M}^{panel}\mathbf{q}+\mathbf{K}^{panel}\mathbf{q}=\mathbf{0}$. Then, a standard eigenvalue problem is obtained. The quantities η_i^2 are the i-th eigenvalues of the vibrating system, which are related to the free vibration frequencies of the panel $\lambda_i = \eta_i/(2\pi)$, while the corresponding displacement vectors $\mathbf{q}_i$ represent the corresponding i-th shapes of the vibrating system, known as eigenvectors or modal shapes [53]. As well known, natural frequencies and modal shapes are obtained by solving a standard eigenvalue problem and finite amplitude vibrations are possible only if $\det[\mathbf{K}^{panel}-\eta^2\mathbf{M}^{panel}]=0$. Moreover, after the determination of eigenvalues and eigenvectors of the system, the mass and polar inertia participation factor of each eigenpair respect to out of plane translation and rotations may be determined as $\mathrm{PF}_i^r=(\mathbf{q}_i^T\mathbf{M}^{panel}\mathbf{r})^2/(\mathbf{r}^T\mathbf{M}^{panel}\mathbf{r})$, where $\mathbf{r}$ is the vector of displacement for the r-th degree of freedom considered. Such factors turn out to be very important for selecting eigenpairs that activate the largest percentage of mass in y_3 direction and for evaluating the rotatory inertia activated by each vibrating mode.

3 Continuous models

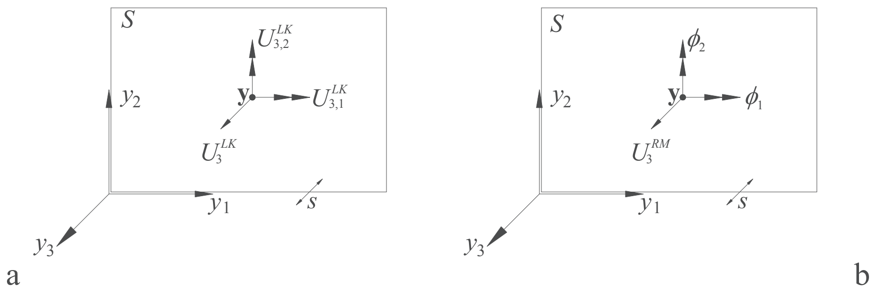

Figure 2. Love-Kirchhoff (a) and Reissner-Mindlin (b) plate models.

Cecchi and Sab [20,24] developed Love-Kirchhoff and Reissner-Mindlin plate models (Figure 2 a,b respectively) for studying masonry walls, in and out of plane loaded, by means of rigorous homogenisation procedures. It is worth noting that in this field of analysis two scale parameters may be taken into account. Considering a masonry assemblage with overall size L, the first scale parameter is the in plane one $\varepsilon = b/L$ that is typical of materials with an internal structure and plane heterogeneity, whereas the second scale parameter is the out of plane one $\zeta = s/L$, that is typical of plate structures and that in general does not depend on in plane heterogeneity. It is well-known that when ζ tends to zero, the 3D solution converges to the Love-Kirchhoff solution. Caillerie [55] has extended this result to periodic plates.

3.1 Love-Kirchhoff plate model

Following Cecchi and Sab [24], in the Love-Kirchhoff orthotropic plate model (Figure 2a) the 3D displacement field is expressed in terms of the out of plane displacement $U_3^{LK}(y_1, y_2)$ as follows:

$$\mathbf{u}^{LK}(\mathbf{y}) = \{-U_{3,1}^{LK}(y_1, y_2)y_3 \quad -U_{3,2}^{LK}(y_1, y_2)y_3 \quad U_3^{LK}(y_1, y_2)\}^T \quad \forall \mathbf{y}, \tag{12}$$

where < , > indicates derivation with respect to a direction of the coordinate system adopted. An identification between the 3D DRBM and the Love-Kirchhoff plate model may be performed as

$$\mathbf{q}^{i,j} = \{u_3^{i,j} \ \omega_2^{i,j} \ \omega_1^{i,j}\}^T = \{U_3^{LK}(\mathbf{y}^{i,j}) \quad -U_{3,1}^{LK}(\mathbf{y}^{i,j}) \quad U_{3,2}^{LK}(\mathbf{y}^{i,j})\}^T. \tag{13}$$

Then, the elastic constants which relate the plate bending tensor $\mathbf{X}$ to the curvature tensor may be highlighted as follows:

$$\mathbf{X} = \begin{Bmatrix} X_{11} \\ X_{22} \\ X_{12} \end{Bmatrix} = \begin{bmatrix} D_{1111} & D_{1122} & 0 \\ D_{1122} & D_{2222} & 0 \\ 0 & 0 & D_{1212} \end{bmatrix} \begin{Bmatrix} \chi_{11} \\ \chi_{22} \\ \chi_{12} \end{Bmatrix}, \tag{14}$$

where $\chi_{\alpha\beta} = -U_{3,\alpha\beta}^{LK}$ with $\alpha,\beta = 1{,}2$ and $D_{\alpha\beta\gamma\delta}$ were identified in the work of Cecchi and Sab [20]. In order to study the free vibrations of the homogenised Love-Kirchhoff plate, Equation (14) needs to be solved together with the following equilibrium equations:

$$\begin{aligned} & M_{\alpha\beta,\beta} - Q_\alpha = 0, \\ & Q_{\alpha,\alpha} - \gamma s\,(\partial^2 U_3^{LK} / \partial t^2) = 0, \end{aligned} \tag{15a,b}$$

where Q_α with α = 1,2 is the generic component of the shear stress tensor $\mathbf{Q} = \{Q_1 \ Q_2\}^T$ and γ has been introduced in paragraph 2.2 for representing masonry density. Therefore, the differential equation of the Love-Kirchhoff plate is obtained and it is given by the following expression:

$$D_{1111}U_{3,1111}^{LK} + 2(D_{1122} + 2D_{1212})U_{3,1122}^{LK} + D_{2222}U_{3,2222}^{LK} = \gamma s \frac{\partial^2 U_3^{LK}}{\partial t^2}. \tag{16}$$

The solution of the equation above is described in appendix B.1 for the determination of homogenised plate frequencies.

3.2 Reissner-Mindlin plate model

The Reissner-Mindlin orthotropic plate model (Figure 2b) proposed by Cecchi and Sab [24] is adopted here for taking into account shear effects in the continuous model. In this model, the 3D displacement field depends on the out of plane displacement $U_3^{RM}(y_1, y_2)$ and two rotations $\phi_1(y_1, y_2), \phi_2(y_1, y_2)$ as follows:

$$\mathbf{u}^{RM}(\mathbf{y}) = \{\phi_1(y_1, y_2)y_3 \quad \phi_2(y_1, y_2)y_3 \quad U_3^{RM}(y_1, y_2)\}^T \quad \forall \mathbf{y}. \tag{17}$$

Similarly to the previous model, an identification between the 3D DRBM and the Reissner-Mindlin plate model is defined as

$$\mathbf{q}^{i,j} = \{u_3^{i,j}\ \omega_2^{i,j}\ \omega_1^{i,j}\}^T = \{U_3^{RM}(\mathbf{y}^{i,j}) \quad \phi_1(\mathbf{y}^{i,j}) \quad -\phi_2(\mathbf{y}^{i,j})\}^T. \tag{18}$$

The bending elastic constants of the model are coincident to those of the Love-Kirchhoff one in Equation (14) by assuming $\chi_{\alpha\beta} = (\phi_{\alpha,\beta} + \phi_{\beta,\alpha})/2$ with α,β = 1,2; whereas the relationship between shear strains and stresses is given by

$$\mathbf{Q} = \begin{Bmatrix} Q_1 \\ Q_2 \end{Bmatrix} = \begin{bmatrix} F_{11} & 0 \\ 0 & F_{22} \end{bmatrix} \begin{Bmatrix} \gamma_{13} \\ \gamma_{23} \end{Bmatrix}, \tag{19}$$

where $\gamma_{\alpha\beta} = \phi_\alpha + U_{3,\alpha}^{RM}$, with α,β = 1,2 and $D_{\alpha\beta\gamma\delta}$ were identified by Cecchi and Sab [24]. In order to study the free vibrations of the homogenised Reissner-Mindlin plate, Equation (14) (with $\chi_{\alpha\beta} = (\phi_{\alpha,\beta} + \phi_{\beta,\alpha})/2$) and Equation (19) needs to be solved together with the following equilibrium equations:

$$\begin{aligned}
&D_{1111}\phi_{1,11} + D_{1212}\phi_{1,22} + (D_{1122} + D_{1212})\phi_{2,12} - F_{11}(\phi_1 + U_{3,1}^{RM}) = I_3 \frac{\partial^2 \phi_1}{\partial t^2}, \\
&(D_{1122} + D_{1212})\phi_{1,12} + D_{1212}\phi_{2,11} + D_{2222}\phi_{2,22} - F_{22}(\phi_2 + U_{3,2}^{RM}) = I_3 \frac{\partial^2 \phi_2}{\partial t^2}, \\
&F_{11}(\phi_{1,1} + U_{3,11}^{RM}) + F_{22}(\phi_{2,2} + U_{3,22}^{RM}) = \gamma s \frac{\partial^2 U_3^{RM}}{\partial t^2}.
\end{aligned} \tag{20a-c}$$

Where $I_3 = \gamma s^3/12$ is the rotatory inertia of the homogenised plate. The solution of the above system of equations is described in appendix B.2. It is worth noting that analytic solutions of homogenised plate models (for both plate types) in static and dynamic fields may be determined for simple load-restraint conditions such as simply supported plates. Then, in the following numerical tests, a simple quadrilateral isoparametric shell element is adopted for representing the homogenised Reissner-Mindlin plate model if analytic solutions do not exist.

4 Numerical tests

A numerical experimentation is performed in order to compare different approaches that may be adopted for modelling the out of plane behaviour of masonry panels and to evaluate their field of applicability. Particular attention is given to the evaluation of the effectiveness of the homogenised models and particular attention is given to the use of discrete model for static and modal analysis. Moreover, the sensitivity of masonry out of plane behaviour to in and out of plane size of heterogeneity and to block dimension ratio is taken into account.
The following models/solution methods are adopted for performing numerical tests:
- Discrete Rigid Block Model (DRBM);
- Homogeneous Reissner-Mindlin plate model - analytic solution (RMS);
- Homogeneous Love-Kirchhoff plate model - analytic solution (LKS);
- Homogeneous Reissner-Mindlin FE model (FEM RM);
- Heterogeneous full 3D FE model (FEM Het).

DRBM and homogeneous plate models have been described in Paragraph 2; the Heterogeneous full 3D FE model is created by means of a commercial FEM code and it is characterised by 6-noded brick elements used for modelling both blocks and mortar joints by adopting different elastic parameters in order to represent the rigid block assumption (block elastic modulus 10^4 times larger than mortar elastic modulus). A masonry panel with a running bond texture pattern is considered as reference case for the following numerical tests (Figure 3). It is characterised by 6 blocks in horizontal direction and 16 courses in vertical direction, with blocks having dimensions b = 250 mm, a = 55 mm and s = 120 mm. Horizontal and vertical mortar joints have the same thickness e = 10 mm, hence, the overall dimensions of the panel are: length L = 1560 mm, height H = 1040 mm and thickness s = 120 mm. The mechanical characteristics of the mortar are E^m = 1000 MPa and ν^m = 0.2.

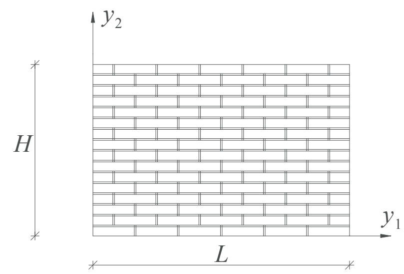

Figure 3. Masonry panel considered for the numerical examples

In the following, two panel boundary conditions are considered: panel simply supported along its edges and panel with fixed base. The first boundary condition is considered in order to provide also analytical solutions that may be determined for the homogeneous plate models considered in this work, moreover such boundary condition may represent a masonry wall restrained along horizontal edges by slabs and along vertical edges by orthogonal walls without a perfect connection. The second boundary condition is considered in order to take into account a realistic restraint for a masonry wall with a base foundation.

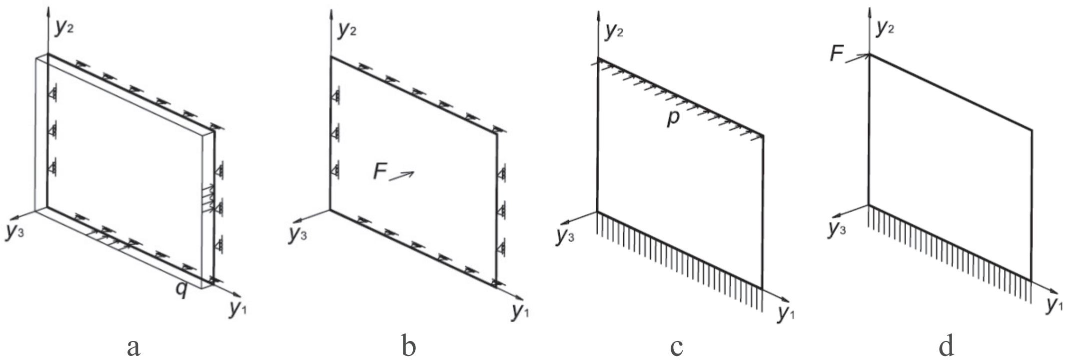

Figure 4. Case studies considered for the static analysis

4.1 Static analysis

In order to perform linear static analysis, several load conditions are taken into account together with the two boundary conditions defined previously. The following list collects the case studies considered (Figure 4):

- Case study 1: panel simply supported along edges, subject to a uniform load distribution (Figure 4a);
- Case study 2: panel simply supported along edges, subject to a load distribution over a small area at its centre (Figure 4b);
- Case study 3: panel with fixed base, subject to a uniform load distribution along upper edge (Figure 4c);
- Case study 4: panel with fixed base, subject to a load distribution over a small area at its upper-left corner (Figure 4d).

All cases are obviously characterised by load distributions acting in the direction orthogonal to the middle plane of the panel. Cases 3 and 4 may represent walls in a masonry building that are perfectly connected only with a slab or foundation element at their base, and that are subject to horizontal forces at their top, transmitted by a well-connected roof (Case 3) or a single beam of a wooden roof (Case 4).

Before performing numerical tests related to the evaluation of scale factor effects and to the comparison of the numerical models proposed, the following figures 5 and 6 collect the deformed shapes together with the maps of out of plane displacements and rotations obtained with the reference panel for the four case studies considered, modelled with the discrete model. Due to the restraint condition of cases 3 and 4, out of plane rotations turn out to be negligible with respect to out of plane translations, whereas for case studies 1 and 2 all block displacement components turn out to be relevant.

4.1.1 Influence of in plane size of heterogeneity – case studies 1,2

The effect of size of heterogeneity on the out of plane behaviour of masonry has been already presented in the recent work of Baraldi et al. [48]. In this work, the in plane scale factor is defined as $\varepsilon = b/L$ (hence, reference panel in Figure 3 is characterised by $\varepsilon = 1/6$) and in this paragraph block dimension ratio is maintained fixed as well as the ratio between the overall dimensions of the panel. For simplicity, an inverse expression of the scale factor $\rho_1 = L/b = 1/\varepsilon$ is also introduced in order to represent with integers the results of the following analyses.

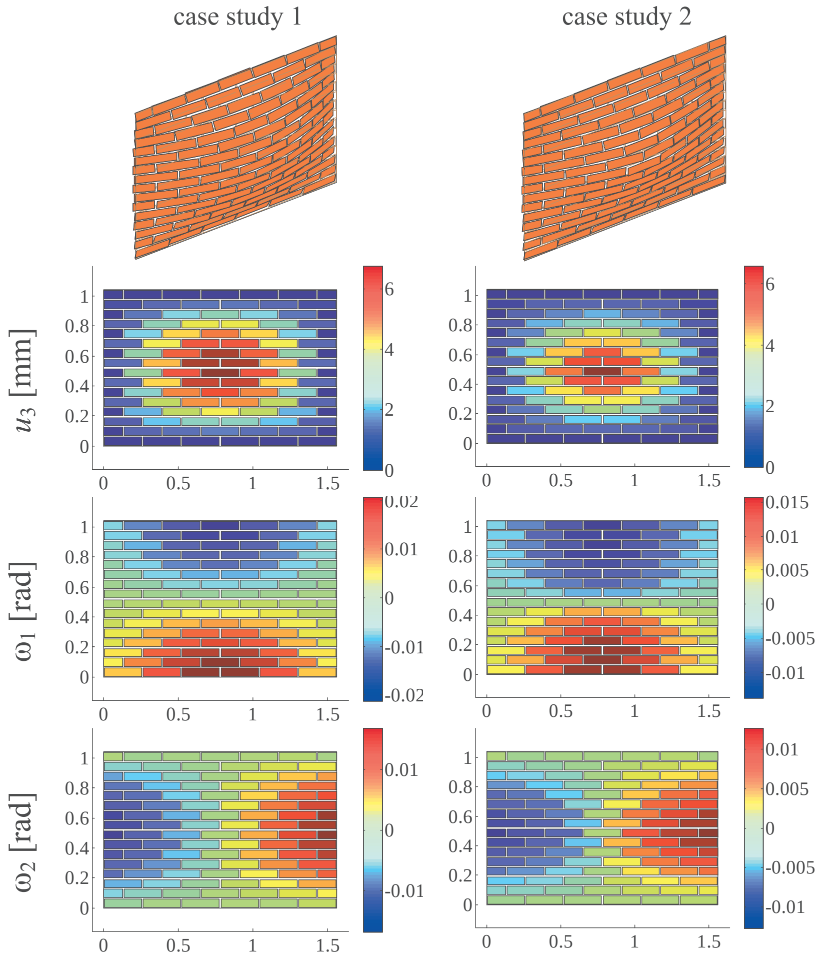

Figure 5. Out of plane displacements and rotations for case studies 1 and 2 applied to the reference panel modelled with the discrete model

Figure 7 shows the maps out of plane displacements obtained for case study 1, considering two different scale factors $\varepsilon = 1/6$ and $\varepsilon = 1/24$, corresponding to ρ_1 equal to 6 and 24, respectively, and adopting DRBM, Love-Kirchhoff solution (LKS) and Reissner-Mindlin solution (RMS). Following the work of Cecchi and Sab [24], analytic solutions for both Love-Kirchhoff and Reissner-Mindlin homogenised plate models may be determined for different load distributions over panels with simple supported edges by means of a Navier double sine series expansion. The order of magnitude of displacements is the same for the models considered, in particular DRBM results are close to Reissner-Mindlin solution for decreasing in plane scale factor ε. Assuming maximum displacements obtained with DRBM as reference solution, differences with respect to results determined with other models are evaluated: $\mathrm{diff} = |u_3^i - u_3^{\mathrm{DRBM}}| / u_3^{\mathrm{DRBM}} \cdot 100$, where i represents a model/solution method adopted (LKS, RMS, FEM RM, FEM Het) and u_3 is evaluated at panel midpoint. Figure 8 shows such differences for increasing ρ_1 and decreasing ε, denoting that solutions determined with all models converge to DRBM solution and in general FEM Het turns out to have a behaviour very close to that of DRBM.

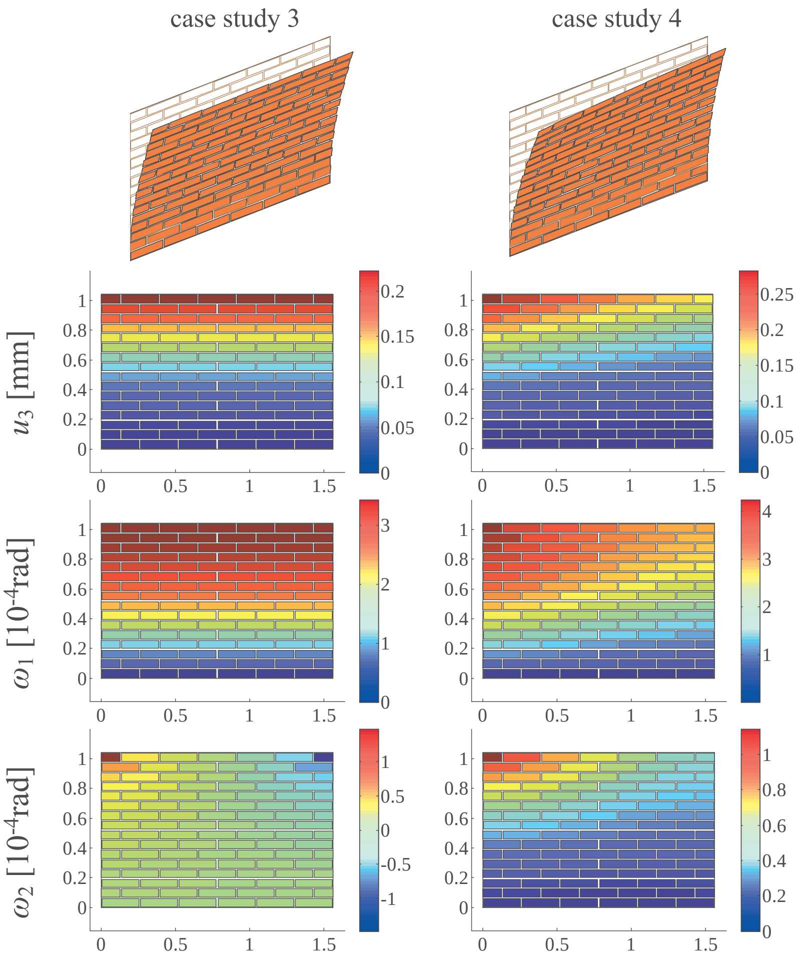

Figure 6. Out of plane displacements and rotations for case studies 3 and 4 applied to the reference panel modelled with the discrete model

For both case studies, FEM Het is more rigid than DRBM, with differences less than 5%, whereas for case study 1 homogeneous models are more deformable with respect to DRBM and differences are less than 5% only for 1/ε > 15. Considering case study 2, all models converge to DRBM solution for decreasing in plane scale factor or increasing $\rho_1 = 1/\varepsilon$ and in particular the Reissner-Mindlin analytic solution presents almost uniform differences with respect to DRBM. As can be expected, FEM RM is more deformable than the corresponding analytic solution. It is worth noting that for both case studies and $1/\varepsilon = 3$, all models present large differences with respect to DRBM; in this case panel thickness is not negligible with respect to panel size (s almost equal to $L/6$), then plate models fail to represent correctly the 3D behaviour of the structure.

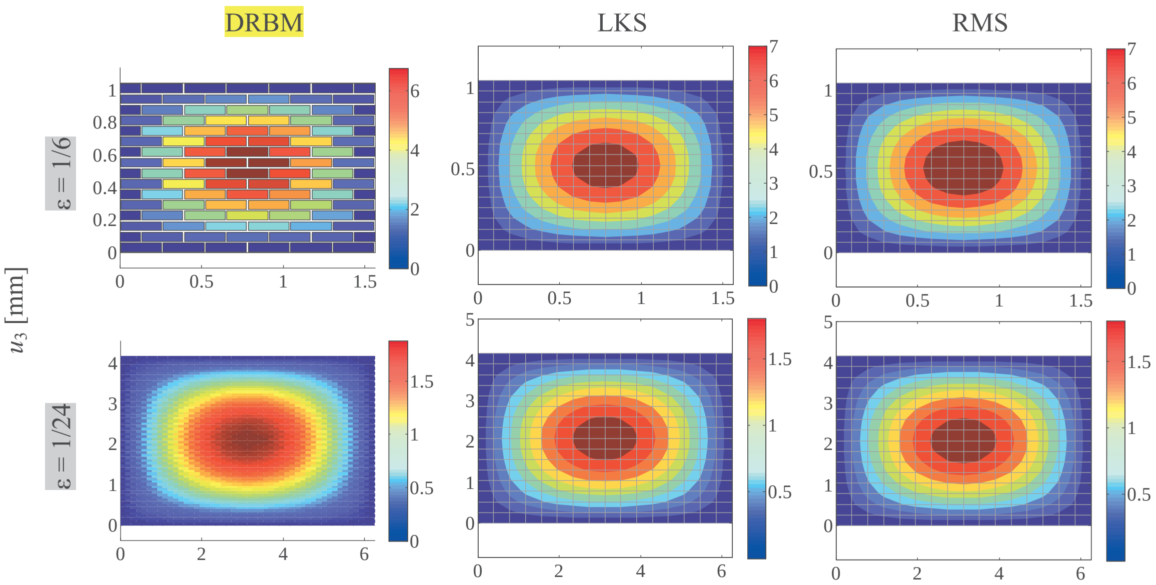

Figure 7. Out of plane displacements for case study 1

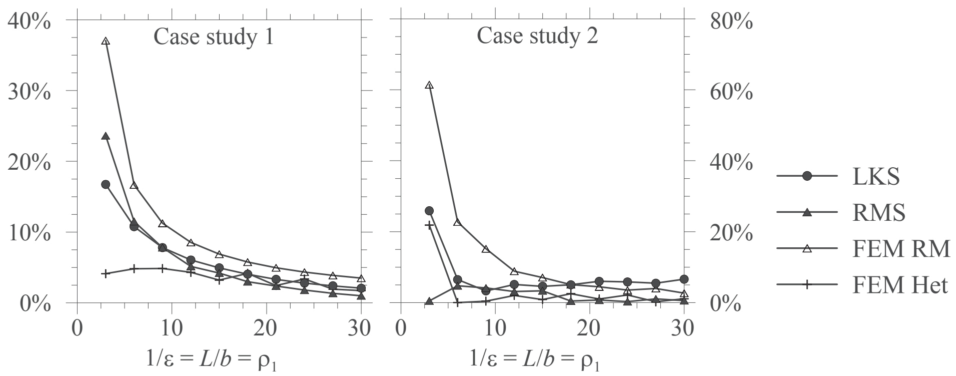

Figure 8. Differences in the determination of maximum panel displacement with respect to DRBM results for varying in plane scale factor

Furthermore, it is possible to compare computation times for each modelling method and for increasing in plane scale factor. Given that load and restraint conditions do not influence computation times, only case study 1 is considered for this comparison and A PC equipped with an Intel Core i7-3770 @ 3.40 GHz and 8 GB RAM is used for this purpose and analyses with 3D heterogeneous FEM are done with a rough mesh refinement with one element along mortar joint thickness in order to avoid huge computation times. For this reason, Figure 9 shows that computation times with the discrete model are generally less than those spent with FEM Het, but they tend to converge for increasing ρ_1. The homogeneous FE model has the advantage that the same mesh refinement, i.e. the same number of degrees of freedom, is adopted for increasing in plane scale factor, hence the computation time is constant and, adopting 32 subdivisions along both plane directions, it turns out to be smaller than that of DRBM for $\rho_1 > 10$.

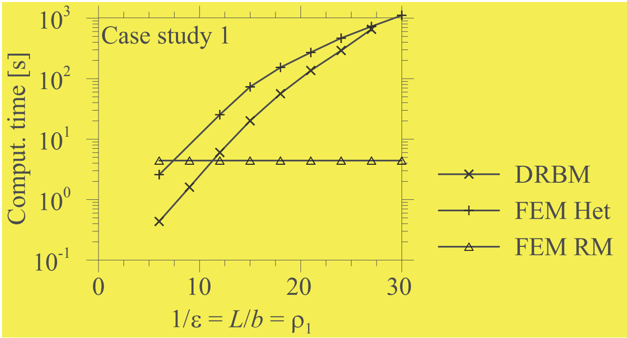

Figure 9. Computation times for varying in plane scale factor

4.1.2 Influence of in plane size of heterogeneity – case studies 3,4

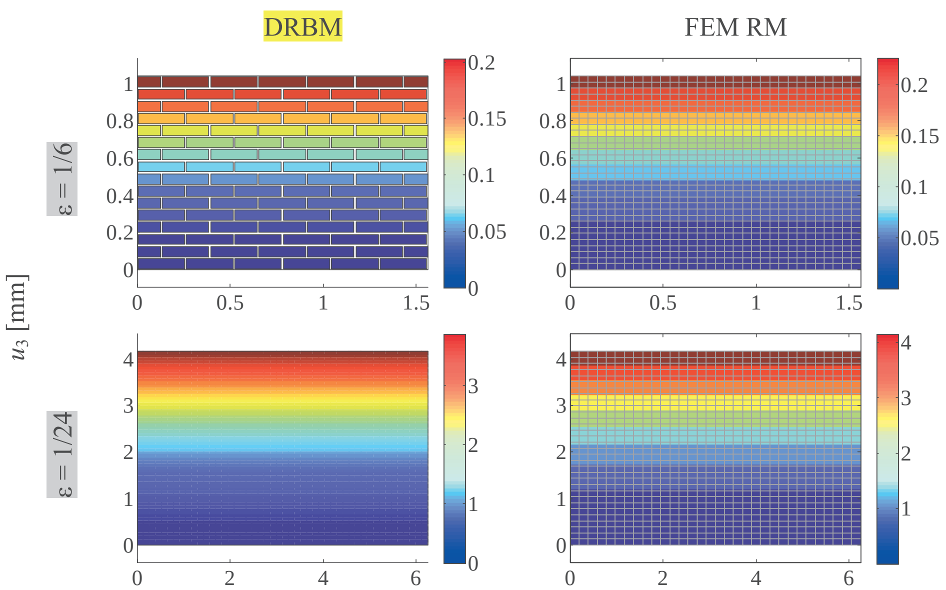

Figure 10. Out of plane displacements for case study 3

In these cases, analytic solutions for homogeneous models do not exist, then the FE model introduced for representing the behaviour of the Reissner-Mindlin plate (FEM RM) turns out to be fundamental for comparing discrete and homogenised approaches of analysis. Figures 10 and 11 show out of plane displacements obtained for case studies 3 and 4, respectively, considering two different scale factors ε = 1/6 and ε = 1/24 and adopting DRBM and FEM RM. Similarly to the previous cases, the order of magnitude of displacements is the same for the numerical models considered, in particular for decreasing the scale factor ε or increasing ρ_1.

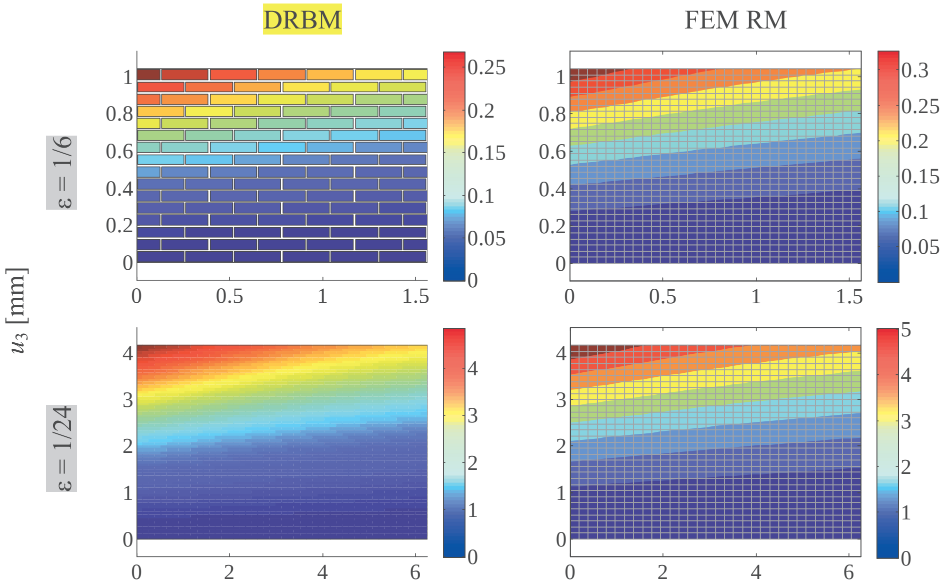

Figure 11. Out of plane displacements for case study 4

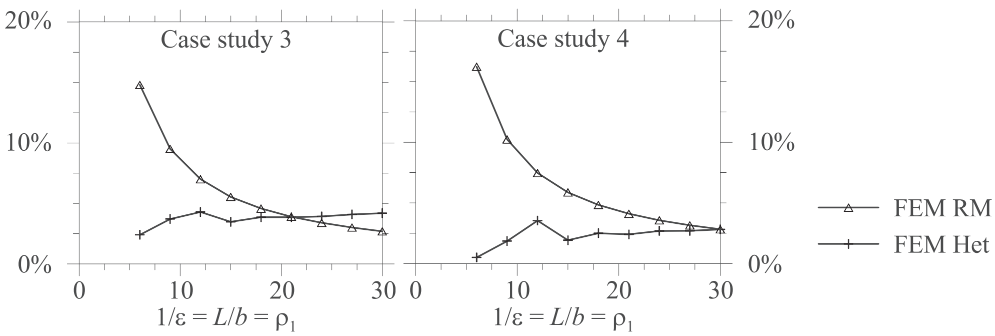

Figure 12. Differences in the determination of maximum panel displacement with respect to DRBM results for varying in plane scale factor

Then, assuming maximum displacements obtained with DRBM as reference, differences with respect to results determined with other models are evaluated for increasing ρ_1 and represented in Figure 12. Similarly to the previous cases, the FEM introduced for representing the Reissner-Mindlin model is more deformable with respect to DRBM and differences are less than 5% only for $\rho_1 > 15$. The 3D heterogeneous FEM is generally more rigid than the DRBM (except for $\rho_1 = 18$ and 24) and differences are always close to 5%.

4.1.3 Influence of out of plane size of heterogeneity: panel thickness

In order to evaluate the effect of panel thickness on the out of plane behaviour of masonry, the out of plane scale factor $\zeta = s/L$, introduced previously, is here considered (for instance, the panel in Figure 3 is characterised by $\zeta = 0.077$). Small values of ζ represent thin panels, whereas large values of ζ represent thick panels. In the following tests, a panel with $\rho_1 = 18$ is considered and its thickness is varied assuming several values of ζ. For simplicity only case studies 1 and 3 are taken into account.

Figure 13 shows maximum panel displacements obtained with both plate models and DRBM for increasing ζ. Considering case study 1, it is evident that the results of both plate models, as expected, converge to DRBM results for small values of ζ, whereas for increasing ζ, both plate models are not able to represent the DRBM; however, as can be expected, the Reissner-Mindlin model is slightly closer to DRBM than the Love-Kirchhoff model. Considering case study 3, Figure 13 shows that differences between DRBM and FEM RM results are almost uniform for increasing ζ, close to 5% (obtained previously in Figure 12 for $\rho_1 = 18$).

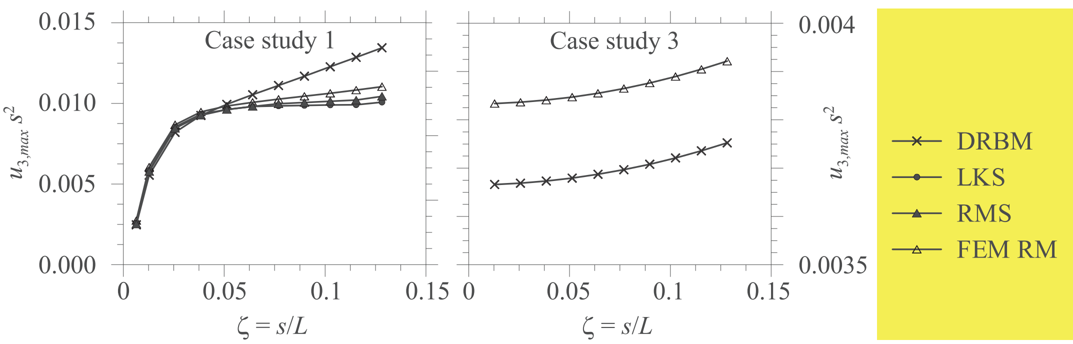

Figure 13. Maximum panel displacements for increasing out of plane scale factor

4.2 Modal analysis

In this paragraph, modal analysis of masonry panels modelled with DRBM is performed in order to evaluate the effectiveness of the model in the determination of out of plane panel vibration frequencies and of the corresponding modal shapes and in order to evaluate the effects of in and out of plane scale factors, together with block and panel dimension ratios.

4.2.1 Panel with simply supported edges

The panel with simply supported edges adopted for case studies 1 and 2 (Figure 4 a,b) is taken into account for first. Figure 14 shows the first four mode shapes and the corresponding frequencies for the reference panel; block thickness is not represented for simplicity and the corresponding colour maps of out of plane displacement are added for better understanding block displacements. Similarly to isotropic plates, first mode shape is characterised by one half-wave in both plane directions, second mode shape has one half wave in y_1 direction and 2 half waves in y_2 direction, third mode shape has 2 half waves in y_1 direction and one half-wave in y_2 direction, fourth mode shape has 2 half-waves in both plane directions.

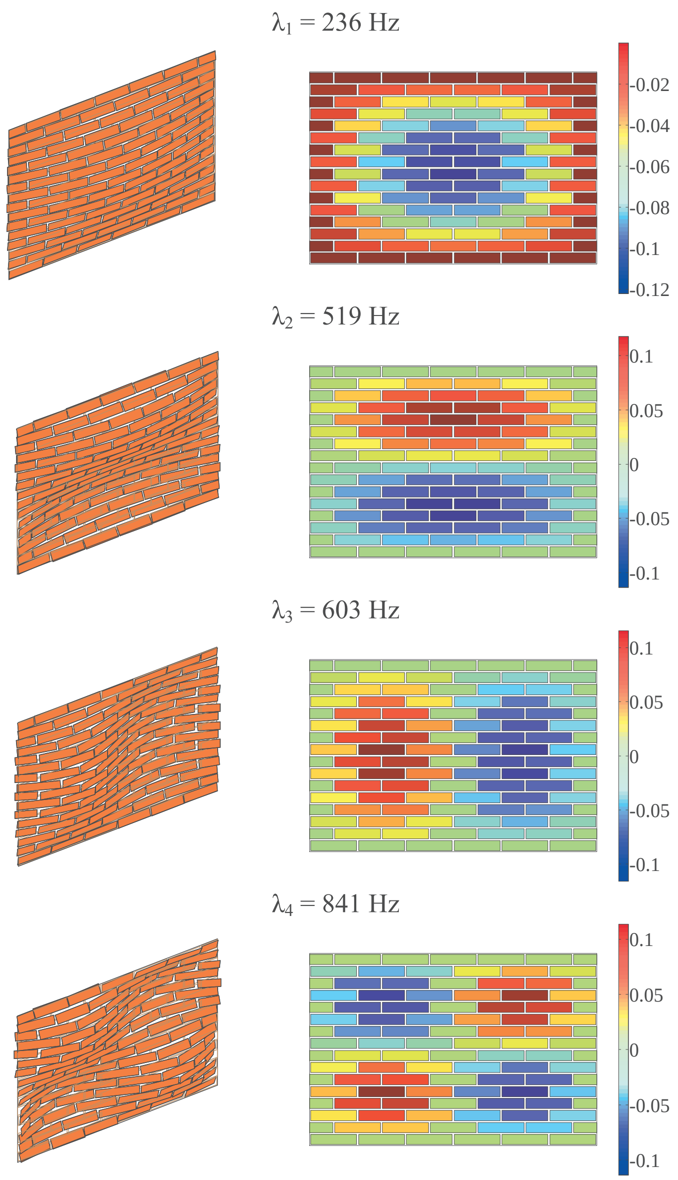

Figure 14. First four mode shapes, maps of out of plane displacements and corresponding frequencies for a simply supported masonry panel taken as reference (Figure 3) and modelled with the discrete model

Analytic solutions for both Love-Kirchhoff and Reissner-Mindlin homogeneous plates may be determined by solving the corresponding equation of motion (Eqs. 16 and 20 a-c, respectively). In appendix B, analytic expressions for frequencies are determined, in order to compare the corresponding results with respect to DRBM results. Figure 15 shows differences $\mathrm{diff}_i^j = (\lambda_i^j - \lambda_i^{\mathrm{DRBM}}) / \lambda_i^{\mathrm{DRBM}} \cdot 100$ in the determination of the first four frequencies assuming DRBM results as references, where j indicates a homogeneous plate solution method or solutions obtained with heterogeneous FEM and i indicates the i-th eigenpair considered. Frequencies obtained with LKS and RMS appear to be quite close to each other and present similar differences with respect to DRBM results. Hence for both analytical models, differences obtained for 1st and 4th frequencies decrease to 2% for decreasing in plane scale factor ε or increasing ρ_1, whereas differences obtained for 2nd and 3rd frequencies slightly decrease for increasing ρ_1 and are close to 10%. Similarly to the static case, the results obtained with the 3D heterogeneous FEM are closer do DRBM results with respect to homogeneous plate solutions.

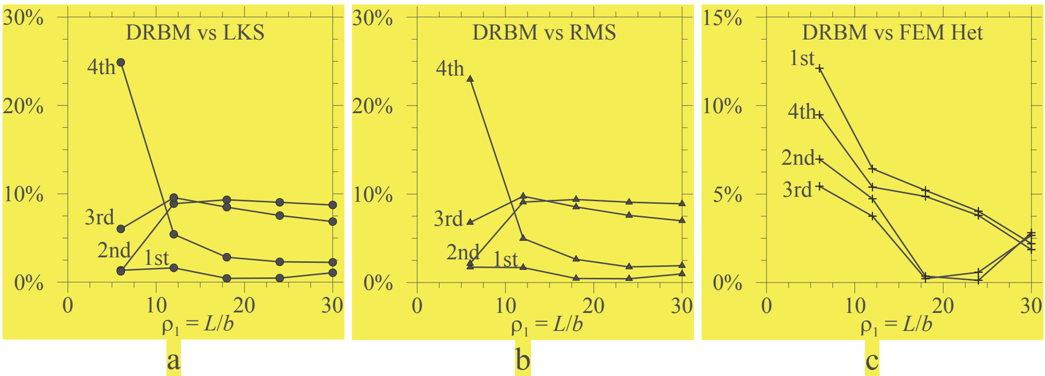

Figure 15. Differences in the determination of panel frequencies with respect to DRBM results for increasing ρ_1 or decreasing in plane scale factor ε

4.2.2 Panel with fixed base

In this paragraph, the panel with fixed base adopted for case studies 3 and 4 (Figure 4 c,d) modelled with DRBM is taken into account. Panel texture in Figure 3 is assumed as reference case, then several geometrical parameters are modified in order to evaluate their effect on panel frequencies and modal shapes. For the following analyses a second in plane ratio $\rho_2 = H/a$ is introduced in order to evaluate block dimension ratio a/b.

Then, the following aspects are considered for performing modal analysis:

- sensitivity to in plane scale factor: maintaining fixed block dimensions, the number of blocks in both plane directions is increased;
- sensitivity to out of plane scale factor: maintaining fixed block and panel dimensions (reference case), the effect of varying panel thickness is taken into account;
- sensitivity to block dimension ratio - subcase 1: maintaining fixed panel dimensions and block height a, the effect of varying block width b is taken into account;
- sensitivity to block shape factor - subcase 2: maintaining fixed panel dimensions and block width b, the effect of varying block height a is taken into account;
- sensitivity to panel shape factor: maintaining fixed block dimensions and panel width L, the effect of varying panel height H is taken into account.

The first row of Figure 16 shows the first four mode shapes of the reference case together with the corresponding frequencies. The first mode shape is characterised by the classical flexural deformation in vertical direction with one half-wave and almost 60% of participant mass in out of plane direction ($PF_1^{u_3} = 59.3\%$). The second mode shape is characterised by a torsional deformation; in this case the participant mass in out of plane direction is close to zero, whereas a participant rotatory inertia with respect to vertical direction ($PF_2^{\omega_1} = 2.2\%$) is obtained. The third mode shape is characterised by a flexural deformation with two half-waves and a $PF_3^{u_3} = 18.6\%$. The fourth mode shape is characterised by flexural deformations in both plane directions (flex. 2D) but mass and rotatory inertia participation factors are close to zero.
In order to evaluate the effect of in plane scale factors, the second row of Figure 16 shows the first four mode shapes and the corresponding frequencies of a panel having $\varepsilon = 1/24$, corresponding to $\rho_1 = 24$ and $\rho_2 = 64$. Mode shapes order does not vary with respect to the reference case, whereas frequencies are smaller than those of the reference case due to the larger deformability of the panel given by the large number of blocks and joints considered. Mass participation factors in out of plane direction of first and third mode shapes are almost coincident to those of the reference case ($PF_1^{u_3} = 60.1\%$, $PF_3^{u_3} = 18.6\%$). Then, in plane scale factor does not affect significantly modal shapes and mass participation factors of fixed base panels. Figure 17a, indeed, shows that frequencies decrease linearly and mode order do not vary for increasing ρ_1 or decreasing ε.
In order to evaluate the effect of out of plane scale factor, Figure 17b shows the first four frequencies for increasing out of plane factor ζ. As can be expected, frequencies increase linearly for increasing ζ due to the increasing stiffness of the panel given by its thickness, moreover mode order does not vary for increasing ζ with respect to the reference case and for this reason deformed shapes are not added to Figure 16. In order to evaluate block dimension ratio a/b, the third row of Figure 16 shows the first four mode shapes and the corresponding frequencies for a panel having $\rho_1 = 24$ and $\rho_2 = 16$, corresponding to $a/b = 1.0$. It is clear that the first mode shape and the corresponding frequency is quite close to the first eigenpair of the reference case, however the subsequent mode shapes are characterised by different order and frequency values with respect to the reference case. Figure 17c, indeed, shows that the first frequency value does not vary significantly for increasing ρ_1 and similarly, the frequency values corresponding to the flexural mode shape with two half-waves are almost constant or slightly increase for increasing ρ_1. On the other hand, frequencies corresponding to torsional mode shape and the one with flexure in both plane directions decrease for increasing ρ_1 due to the increasing deformability given by the increasing number of blocks and mortar joints in horizontal direction. Hence, it is clear that flexural mode shapes are not affected significantly by scale factor ρ_1 if block height and panel dimensions are fixed. Continuing to consider the effect of block dimension ratio a/b, the fourth row of Figure 16 shows the first four mode shapes of a panel having $\rho_1 = 6$ and $\rho_2 = 32$, corresponding to $a/b = 0.125$.

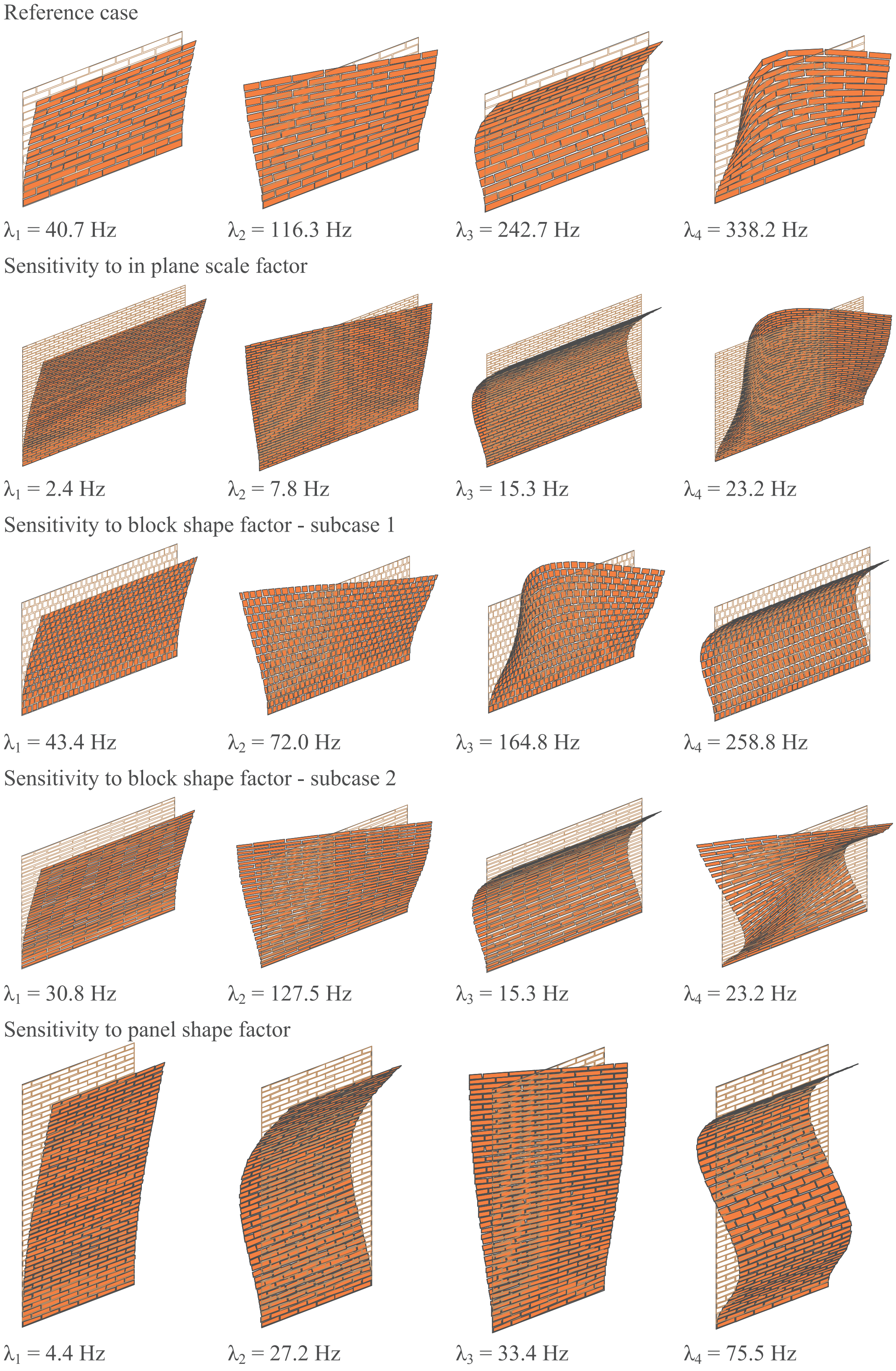

Figure 16. Modal analysis of masonry panels (DRBM) varying several parameters

First and third mode shapes are characterised by flexural deformation with one and two half-waves, respectively, whereas second mode shape is a simple torsional deformation and the fourth mode shape is a combined flexural-torsional deformation. Frequencies corresponding to flexural modal shapes decrease for increasing ρ_2 (Figure 17d), whereas frequencies corresponding to torsional modal shapes initially decrease up to $\rho_2 = 10$ and then increase for $i\rho_2 > 10$.

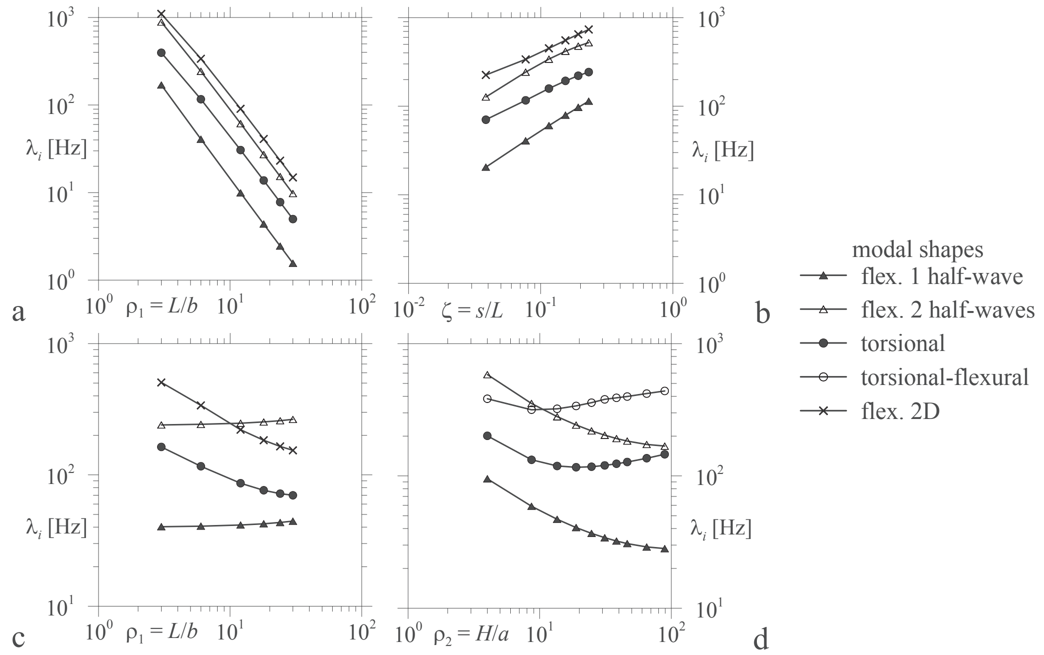

Figure 17. First four panel frequencies varying in plane and out of plane scale factors. Sensitivity to: in plane scale factor (a), out of plane scale factor (b); block shape factor - subcase 1 (c), block shape factor - subcase 2 (d)

Finally, the effect of panel shape factor is considered by varying *L*/*H* ratio. For example, the fifth row of Figure 16 collects the first four modal shapes corresponding to $L/H = 0.5$, with $\rho_1 = 6$. Thanks to the slenderness of the panel, first, second and fourth mode shapes are flexural with one, two and three half-waves, respectively, whereas the third modal shape is torsional. Figure 18a shows frequency values for increasing *L*/*H*. For the range of *L*/*H* values considered, the first mode shape is always flexural with one half-wave and it is possible to define an expression for estimating frequency values linearly depending on *L*/*H* and panel material parameters. Moreover, Figure 18b shows mass participation factors related to this case study and the first mode shape tends to activate the 60% of the total panel mass for decreasing *L*/*H*, whereas the percentage of mass activated by the second flexural mode shape does not depend on *L*/*H* and it is close to 20%. Figure 18c shows rotatory inertia participation factors, that are strictly related to block out of plane rotations. In particular, the rotatory inertia related to ω_2 for the first and second flexural modes increases significantly for increasing *L*/*H*.

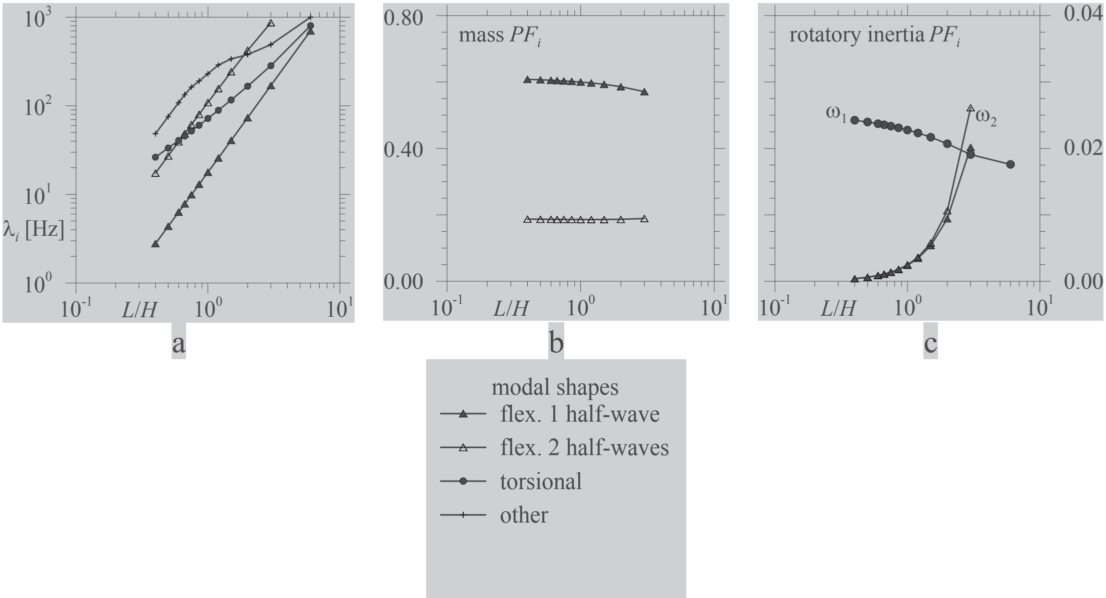

Figure 18. Modal analysis varying panel shape factor L/H. Frequency values (a), mass participation factors (b); rotatory inertia participation factors (c)

4 Conclusions

In this work the out of plane behaviour of masonry panels with regular texture has been considered. Elastic behaviour, small displacements, and fixed contact topology are the hypotheses adopted for the analysis. Several numerical and analytical models have been taken into account for modelling masonry, with particular attention to a simple discrete model introduced by Cecchi and Sab [24] and here extended by performing static analysis with several boundary conditions and load cases and, in particular, by performing out of plane modal analysis. The proposed review has shown that the discrete model (DRBM) is simple, effective and efficient for modelling out of plane behaviour, thanks to the small number of degrees of freedom involved during the analyses. Such simplicity allowed to define the stiffness matrix of the regular assemblage of blocks, in order to obtain fast static solutions with respect to the molecular dynamics method adopted originally and in order to perform modal analysis by solving eigenvalue problems.

Both in static and modal analysis, the 3D Heterogeneous FEM turned out to be quite close to the DRBM, however it is affected by the large number of degrees of freedom needed for modelling accurately the masonry structure and by the mesh refinement required for obtaining accurate results. Love-Kirchhoff and Reissner-Mindlin homogeneous plate models turned out to be more deformable than the DRBM almost in all case studies considered in static and modal analysis. However, performing static analysis, analytic solutions obtained with the Reissner-Mindlin plate turned out to be closer to DRBM for decreasing in plane scale factor. In general, for the four case studies considered during static analysis tests, the

homogeneous models proved to be effective for representing masonry behaviour only for small values of the in plane scale factor (i.e. $\varepsilon < 1/15$ or $\rho_1 > 15$).
The FEM adopted for modelling the Reissner-Mindlin homogeneous plate for static analysis turned out to be slightly more deformable than the corresponding analytical model, however it has been fundamental in the determination of out of plane displacements for the case studies of panels with fixed base. Furthermore, computation times with FEM RM are not affected by the in plane scale factor, hence this model may be successfully adopted in case of panels with a large number of blocks.
Then, modal analysis performed for the simply supported plate allowed authors to define the analytic solutions in terms of frequencies for Love-Kirchhoff and Reissner-Mindlin homogeneous plate models. Similarly to the static analysis case, homogeneous models turned out to be effective for representing masonry behaviour only for small values of the in plane scale factor (i.e. $\varepsilon < 1/15$ or $\rho_1 > 15$). Further modal analyses on masonry panels with fixed base have been carried on adopting only discrete model, obtaining flexural deformation with one half-wave as first mode shape and obtaining often torsional deformation as second mode shape. In plane and out of plane scale factors turned out to slightly influence mode shapes order.
Further developments of this work will regard the extension of the DRBM to the field of nonlinear analysis by assuming rigid block and nonlinear interfaces, similarly to recent developments performed by authors in plane case [50]. Furthermore, more accurate continuous models, such as the Cosserat continuum, will be taken into account and compared to the DRBM here reviewed.

Acknowledgements

The research has been carried out thanks to the financial support of PRIN 2015 (under grant 2015JW9NJT_014, project “Advanced mechanical modeling of new materials and structures 664 for the solution of 2020 Horizon challenges”).

References

[1] A.W. Page, "Finite Element Model for Masonry", Journal of the Structural Division, 104(8), 1267-1285, 1978.
[2] S.S. Ali, A.W. Page, "Finite element model for masonry subjected to concentrated loads", Journal of Structural Engineering, 114(8), 1761-1784, 1988. DOI: 10.1061/(ASCE)0733-9445(1988)114:8(1761)
[3] A.D. Tzamtzis, B. Nath, "Application of a Three-dimensional Interface Element to Non-linear Static and Dynamic Finite Element Analysis of Discontinuous Systems", Engineering Systems Design and Analysis Conference, ASME, 1, 219-222, 1992.
[4] A.D. Tzamtzis, P.G. Asteris, "FE Analysis of Complex Discontinuous and Jointed Structural Systems (Part 2: Application of the Method – Development

of a 3D Model for the Analysis of Unreinforced Masonry Walls)", Electronic Journal of Structural Engineering, 1, 93-107, 2004.
[5] P.A. Cundall, "A computer model for simulating progressive large scale movements in blocky rock systems". Proceedings of Symposium of International Society of Rock Mechanics, Nancy, France, 1971.
[6] P.A. Cundall, R.D. Hart, "Numerical modelling of discontinua", Engineering Computations, 9(2), 101-113, 1992. DOI: 10.1108/eb023851
[7] Itasca, "UDEC (Universal Distinct Element Code) Version ICG1.5 User's Manual", 1989.
[8] P.A. Cundall, "Formulation of a Three-dimensional Distinct Element Model Part I. A Scheme to Detect and Represent Contacts in a System Composed of Many Polyhedral Blocks", International Journal of Rock Mechanics and Mining Sciences & Geomechanics Abstracts, 25(3), 107-116, 1988. DOI: 10.1016/0148-9062(88)92293-0
[9] P.A. Cundall, R. Hart, J. Lemos, "Formulation of a Three-dimensional Distinct Element Model Part II. Mechanical Calculations for Motion and Interaction of a System Composed by Many Polyedral Blocks", International Journal of Rock Mechanics and Mining Sciences & Geomechanics Abstracts, 25(3), 117-125 1988. DOI: 10.1016/0148-9062(88)92294-2
[10] Itasca, "3DEC 3-D Distinct Element Code", 1988.
[11] A. Munjiza, D.R.J. Owen, N. Bićanić, "A combined finite-discrete element method In transient dynamics of fracturing solids", Engineering computations, 12(2), 145-174. 1995.
[12] A. Munjiza, "The Finite/Discrete Element Method", John Wiley and Sons, Chicester, England, 2004.
[13] G.H. Shi, "Discontinuous Deformation Analysis: A New Numerical Model for the Statics and Dynamics of Block Systems". PhD Thesis, University of California, Berkeley, USA, 1988.
[14] J. Liu, X. Kong, G. Lin, "Formulations of three-dimensional discontinuous deformation analysis method", Acta Mechanica Sinica, 20(3), 270-282, 2004.
[15] R.G. Mikola, N. Sitar, "Explicit three dimensional discontinuous deformation analysis for blocky system", ARMA - 47th U.S. Rock Mechanics/Geomechanics Symposium, 23-26 June, San Francisco, California, 2013.
[16] J.V. Lemos, "Discrete Element Modeling of Masonry Structures", International Journal of Architectural Heritage: Conservation, Analysis, and Restoration, 1(2), 190-213, 2007. DOI: 10.1080/15583050601176868
[17] K. Bagi, V. Sarhosis, G. Milani, "Computational Modeling of Masonry Structures Using the Discrete Element Method", IGI Global, Hershey, PA, USA, 2016. DOI: 10.4018/978-1-5225-0231-9
[18] R. Masiani, N. Rizzi, P. Trovalusci, "Masonry as structured continuum", Meccanica, 30(6), 673-683, 1995. DOI: 10.1007/BF00986573
[19] G. Formica, V. Sansalone, R. Casciaro, "A mixed solution strategy for the nonlinear analysis of brick masonry walls", Computational Methods in Applied Mechanics and Engineering, 191, 5847-5876. DOI: 10.1016/S0045-7825(02)00501-7

[20] A. Cecchi, K. Sab, "Out of plane model for heterogeneous periodic materials: the case of masonry", European Journal of Mechanics A/Solids, 21, 249-268, 2002. DOI: 10.1016/S0997-7538(02)01243-3
[21] S. Casolo, "Modelling in-plane micro-structure of masonry walls by rigid elements", International Journal of Solids and Structures, 41, 3625-3641, 2004. DOI: 10.1016/j.ijsolstr.2004.02.002
[22] S. Casolo, "Macroscopic modelling of structured materials: Relationship between orthotropic Cosserat continuum and rigid elements", International Joural of Solids and Structures, 43, 475-496, 2006. DOI: 10.1016/j.ijsolstr.2005.03.037
[23] A. Cecchi, K. Sab, "A multi-parameter homogenization study for modeling elastic masonry", European Journal of Mechanics A/Solids, 21(2),. 249-268, 2002. DOI: 10.1016/S0997-7538(01)01195-0
[24] A. Cecchi, K. Sab, "A comparison between a 3D discrete model and two homogenised plate models for periodic elastic brickwork", International Journal of Solids and Structures, 41(9-10), 2259-2276, 2004. DOI: 10.1016/j.ijsolstr.2003.12.020
[25] A. Cecchi, G. Milani, A. Tralli, "Validation of analytical multiparameter homogenization models for out-of-plane loaded masonry walls by means of the finite element method", Journal of Engineering Mechanics, 131(2), 185-198, 2005. DOI: 10.1061/(ASCE)0733-9399(2005)131:2(185)
[26] S. Casolo, "Modelling the out-of-plane seismic behaviour of masonry walls by rigid elements", Earthquake Engineering and Structural Dynamics, 29(12), 1797-1813, 2000. DOI: 10.1002/1096-9845(200012)29:12<1797::AID-EQE987>3.0.CO;2-D
[27] S. Casolo, G. Uva, "Nonlinear analysis of out-of-plane masonry façades: Full dynamic versus pushover methods by rigid body and spring model", Earthquake Engineering and Structural Dynamics, 42(4), 499-521, 2013. DOI: 10.1002/eqe.2224
[28] S. Casolo, G. Milani, "A simplified homogenization-discrete element model for the non-linear static analysis of masonry walls out-of-plane loaded", Engineering Structures, 32(8), 2352-2366, 2010. DOI: 10.1016/j.engstruct.2010.04.010
[29] A. Anthoine, "Derivation of the in-plane elastic characteristics of masonry through homogenization theory", International Journal of Solids and Structures, 32(2), 137-163, 1995. DOI: 10.1016/0020-7683(94)00140-R
[30] R. Masiani, P. Trovalusci, "Cosserat and Cauchy materials as continuum models of brick masonry", Meccanica, 31(4), 421-432, 1996.
[31] J. Sulem, H.B. Mühlhaus, "A continuum model for periodic two-dimensional block structures". Mechanics of Cohesive-Frictional Materials, 2(1), 31–46, 1997.
[32] G. Salerno, G. De Felice, "Continuum modeling of periodic brickwork", International Journal of Solids and Structures, 46(5), 1251-1267, 2009. DOI: 10.1016/j.ijsolstr.2008.10.034

[33] M.L. De Bellis, D. Addessi, "A Cosserat based multi-scale model for masonry structures". International Journal for Multiscale Computational Engineering, 9 (5), 543-563, 2011.

[34] A. Pau, P. Trovalusci, "Block masonry as equivalent micropolar continua: the role of relative rotations". Acta Mechanica, 223(7), 1455-1471, 2012 DOI: 10.1007/s00707-012-0662-8

[35] D. Baraldi, A. Cecchi, A. Tralli, A., "Continuous and discrete models for masonry like material: a critical comparative study", European Journal of Mechanics A/Solids, 50, 39-58, 2015. DOI: 10.1016/j.euromechsol.2014.10.00

[36] I. Stefanou, J. Sulem, I. Vardoulakis, "Three-dimensional Cosserat homogenization of masonry structures: elasticity". Acta Geotechnica, 3, 71–83, 2008. DOI: 10.1007/s11440-007-0051-y

[37] M. Godio, I. Stefanou, K. Sab, J. Sulem, "Dynamic finite element formulation for Cosserat elastic plates", International Journal for Numerical Methods in Engineering, 101(13), 992-1018, 2015. DOI: 10.1002/nme.4833

[38] C. Baggio, P. Trovalusci, "Limit analysis for no-tension and frictional three-dimensional discrete systems", Mechanics of Structures & Machines, 26(3), 287-304, 1998.

[39] N.T.K. Lam, M. Griffith, J Wilson, K. Doherty, "Time-history analysis of URM walls in out-of-plane flexure", Engineering Structures, 25(6), 743-754, 2003. DOI: 10.1016/S0141-0296(02)00218-3

[40] A. Orduña, P.B. Lourenço, "Three-dimensional limit analysis of rigid blocks assemblages. Part II: Load-path following solution procedure and validation", International Journal of Solids and Structures, 42(18-19), 5161-5180, 2005. DOI: 10.1016/j.ijsolstr.2005.02.011

[41] A. Cecchi, G. Milani, A. Tralli, "A Reissner-Mindlin limit analysis model for out-of-plane loaded running bond masonry walls", International Journal of Solids and Structures, 44(5), 1438-1460, 2007. DOI: 10.1016/j.ijsolstr.2006.06.033

[42] G. Milani, P. Lourenço, A. Tralli, "3D homogenized limit analysis of masonry buildings under horizontal loads", Engineering Structures, 29(11), 3134-3148, 2007. DOI: 10.1016/j.engstruct.2007.03.003

[43] A. Cecchi, G. Milani, "A kinematic FE limit analysis model for thick English bond masonry walls", International Journal of Solids and Structures, 45(5), 1302-1331, 2008. DOI: 10.1016/j.ijsolstr.2007.09.019

[44] G. Milani, P.B. Lourenço, "A simplified homogenized limit analysis model for randomly assembled blocks out-of-plane loaded", Computers and Structures, 88(11-12), 690-717, 2010. DOI: 10.1016/j.compstruc.2010.02.009

[45] E. Reccia, A. Cazzani, A. Cecchi, "FEM-DEM Modeling for Out-of-plane Loaded Masonry Panels: A Limit Analysis Approach", Open Civil Engineering Journal, 6(1), 231-238, 2012. DOI: 10.2174/1874149501206010231

[46] G. Milani, M. Pizzolato, A. Tralli, "Simple numerical model with second order effects for out-of-plane loaded masonry walls", Engineering Structures, 48, 98-120, 2013. DOI: 10.1016/j.engstruct.2012.08.029

[47] T.M., Ferreira, A.A. Costa, A. Costa, "Analysis of the Out-Of-Plane Seismic Behavior of Unreinforced Masonry: A Literature Review", International Journal of Architectural Heritage: Conservation, Analysis, and Restoration, 9(8), 949–972, 2015. DOI: 10.1080/15583058.2014.885996

[48] D. Baraldi, A. Cecchi, A. Tralli, "Discrete and Continuous Models for Out-of-Plane Loaded Masonry Like Structures: A Multiscale Comparative Study", in J. Kruis, Y. Tsompanakis, B.H.V. Topping, (Editors), "Proceedings of the Fifteenth International Conference on Civil, Structural and Environmental Engineering Computing", Civil-Comp Press, Stirlingshire, UK, Paper 207, 2015. DOI:10.4203/ccp.108.207

[49] R. Masiani, P. Trovalusci, "Size effects in continuum modelling of brick masonry", Computer Methods in Structural Masonry-3, J. Middleton and G.N. Pande (Eds.), BIJ, Swansea (UK), 42-51, 1995.

[50] D. Baraldi, E. Reccia, A. Cecchi, "DEM & FEM/DEM models for laterally loaded masonry walls", COMPDYN 2015 - 5th ECCOMAS Thematic Conference on Computational Methods in Structural Dynamics and Earthquake Engineering, 2144-2157, 2015.

[51] D. Baraldi, A. Cecchi, "A full 3D rigid block model for the collapse behaviour of masonry walls", European Journal of Mechanics A/Solids, 2017. (in press) http://dx.doi.org/10.1016/j.euromechsol.2017.01.012

[52] D. Baraldi, A. Cecchi, "Discrete and continuous models for the in plane modal analysis of masonry structures", 11th World Congress on Computational Mechanics, WCCM 2014, 5th European Conference on Computational Mechanics, ECCM 2014 and 6th European Conference on Computational Fluid Dynamics, ECFD 2014, 3313-3324, 2014.

[53] R.W. Clough, J. Penzien, "Dynamics of Structures", Computers & Structures, Inc. Berkeley, CA, USA, 1995.

[54] D. Baraldi, A. Cecchi, "Discrete Element Model for in plane loaded viscoelastic masonry", International Journal for Multiscale Computational Engineering, 12(2), 155-175, 2014. DOI: 10.1615/IntJMultCompEng.2014008118.

[55] D. Caillerie, "Thin elastic and periodic plates", Mathematical Methods in the Applied Sciences, 6(1), 159-191, 1984.

[56] M.C. Ferris, F. Tin-Loi, "Limit analysis of frictional block assemblies as a mathematical program with complementarity constraints", International Journal of Mechanical Sciences, 43(1), 209-224, 2001. DOI: 10.1016/S0020-7403(99)00111-3.

[57] A.L. Dobyns, "Analysis of simply-supported orthotropic plates subject to static and dynamic loads", AIAA Journal, 19(5), 642-650, 1981.

Appendix

A Stiffness matrix of a regular block assemblage

In order to describe how to determine the stiffness matrix of a regular masonry assemblage, the simplest procedure envisages the definition of the stiffness matrix for an interface S_{k_1,k_2} between two generic blocks. Then, the degrees of freedom related to the generic block $B_{i,j}$ in Equation (1) have to be taken into account together with the degrees of freedom of a generic neighbour $B_{i+k_1,j+k_2}$:

$$\mathbf{q}^{i+k_1,j+k_2} = \{u_3^{i+k_1,j+k_2} \ \omega_1^{i+k_1,j+k_2} \ \omega_2^{i+k_1,j+k_2}\}^T, \tag{21}$$

where k_1, k_2 = ± 1, for horizontal interfaces, k_1 = ± 2 and k_2 = 0 for vertical interfaces. The degrees of freedom of the couple of adjacent blocks may be collected in the following vector having 6 components:

$$\mathbf{q}^{k_1,k_2} = \{u_3^{i,j} \ \omega_1^{i,j} \ \omega_2^{i,j} \ u_3^{i+k_1,j+k_2} \ \omega_1^{i+k_1,j+k_2} \ \omega_2^{i+k_1,j+k_2}\}^T. \tag{22}$$

Adopting the notation of vectors $\mathbf{q}^{i,j}$ and $\mathbf{q}^{i+k_1,j+k_2}$, Equation (3a-c), representing relative displacements between the blocks, may be written in matrix form as follows:

$$\begin{aligned}\mathbf{d}^{k_1,k_2} = \begin{Bmatrix} d_3^{k_1,k_2} \\ \delta_1^{k_1,k_2} \\ \delta_2^{k_1,k_2} \end{Bmatrix} = \begin{bmatrix} 1 & -k_2 a/2 & k_1 b/4 \\ 0 & 1 & 0 \\ 0 & 0 & 1 \end{bmatrix} \begin{Bmatrix} u_3^{i+k_1,j+k_2} \\ \omega_1^{i+k_1,j+k_2} \\ \omega_2^{i+k_1,j+k_2} \end{Bmatrix} + \\ - \begin{bmatrix} 1 & k_2 a/2 & -k_1 b/4 \\ 0 & 1 & 0 \\ 0 & 0 & 1 \end{bmatrix} \begin{Bmatrix} u_3^{i,j} \\ \omega_1^{i,j} \\ \omega_2^{i,j} \end{Bmatrix} = \mathbf{H}^{i+k_1,j+k_2} \mathbf{q}^{i+k_1,j+k_2} - \mathbf{H}^{i,j} \mathbf{q}^{i,j},\end{aligned} \tag{23}$$

and, assembling matrix and vector components, the following expression may be obtained:

$$\mathbf{d}^{k_1,k_2} = \begin{bmatrix} -\mathbf{H}^{i,j} & 0 \\ 0 & \mathbf{H}^{i+k_1,j+k_2} \end{bmatrix} \begin{Bmatrix} \mathbf{q}^{i,j} \\ \mathbf{q}^{i+k_1,j+k_2} \end{Bmatrix} = \mathbf{H}^{k_1,k_2} \mathbf{q}^{k_1,k_2}. \tag{24}$$

It is worth noting that k_1 and k_2 depend on the interface considered, consequently matrices $\mathbf{H}^{i+k_1,j+k_2}$, $\mathbf{H}^{i,j}$ and then matrix $\mathbf{H}^{k_1,k_2}$ depend on the interface considered.
Moreover, interface forces and couples depend on relative displacements between blocks by means of constitutive relations involving interface stiffness matrices. Then, substituting the equations above in the expression of the elastic energy of the